Using aerial imagery for assessing pasture vegetation coverage[1]

Lucas Gustavo Yock Durante[2]*, Jorge Wilson Cortez[3], Jessica Evangelista de Souza[4], Anamari Viegas de Araújo Motomiya[5], Eber Augusto Ferreira do Prado[6]

ABSTRACT - We aimed to assess pasture vegetation cover over two growing seasons using vegetation indices derived from RDB aerial images acquired by drones and multispectral satellite imagery. The study area was already divided into six grazing paddocks grown with forage grasses, three with *Megathyrsus maximus* cv. Mombaça and three with *Urochloa brizantha* cv. MG-4. Sampling was conducted during the January and July 2022/2023 growing season. The study adopted precision agriculture principles, generating customized sampling grids for each pasture, with an approximate density of four points per hectare. Field data were collected on pasture height, soil-exposed percentage, chlorophyll content, and pasture green biomass. RGB aerial imagery was acquired using a drone, while multispectral data was obtained from the Sentinel 2A satellite four times. Pasture vegetation cover (PVC) was estimated after calculating the vegetation indices Normalized Difference Vegetation Index (NDVI), Green-Red Vegetation Index (GRVI), and Green Leaf Index (GLI). PVC results indicate a slight degree of pasture degradation during the 2022/2023 growing season. Images captured by UAVs (unmanned aerial vehicles) enabled accurate identification of sparse areas prone to degradation, offering valuable insights to enhance pasture and forage management.

Key words: Forage. Drone. Vegetation index. Pasture management.

INTRODUCTION

According to IBGE (2024), at least half of natural pastures are undergoing degradation, primarily due to inadequate management practices. Natural pastures are essential for soil preservation, as their root systems prevent erosion, enhance soil structure, and support efficient nutrient cycling (Andrade *et al.*, 2017). Additionally, forage green cover contributes significantly to carbon sequestration, reducing greenhouse gas emissions and improving air quality (Morais *et al.*, 2018).

Appropriate management methods can mitigate pasture degradation. For instance, continuous stocking allows animals unrestricted access to the entire grazing area without paddocks or rest periods, often leading to pasture stress. In contrast, rotational stocking offers a more efficient approach by alternating grazing and rest periods across different paddocks. This practice promotes pasture recovery, enhances pest control, and increases productivity per unit area (Andrade *et al.*, 2017; Lima *et al.*, 2017).

Effective pasture management requires precise determination of forage mass. Traditional methods involve on-site sampling, drying, and weighing to measure dry mass. Another common approach uses a pasture ruler to estimate height, guiding decisions on animal entry and exit timing. Emerging technologies, such as remote spectral sensors, provide indirect estimations and are particularly advantageous for assessing large areas without *in situ* sampling (Morais *et al.*, 2018).

Remote sensing (RS) technologies are also gaining prominence, using platforms such as satellites, aircraft, remotely piloted aircraft (RPA) systems, and self-propelled agricultural machinery (Weiss *et al.*, 2020). These platforms capture image data, which are processed into vegetation indices (VIs) through mathematical equations. These indices help identify issues within the study area (Hernández-López *et al.*, 2021). Satellite-based sensors are increasingly popular due to their cost-effectiveness and efficiency in large-scale spatial analysis. However, cloud cover can compromise image quality, posing challenges for agricultural applications (Ramadhani *et al.*, 2021). To address this, sensors embedded in RPAs offer an alternative, reducing cloud interference, providing higher spatial resolution, and increasing revisit frequency (Silva, 2020).

Given the critical role of quality pastures in agricultural sustainability and development, efficient assessment and monitoring techniques are essential. Orbital satellite technologies are particularly suited for monitoring medium- to large-scale areas over multiple study periods (Ferreira and Ferreira Neto, 2018; Santos *et al.*, 2018; Themistocleous *et al.*, 2014). Therefore, this study aimed to evaluate pasture vegetation cover over two growing seasons using vegetation indices derived from RGB aerial images captured by UAVs and multispectral satellite images.

MATERIAL AND METHODS

The study was conducted on the 21.22-hectare Buby Dila Ranch, located at 21°47'10.85" S latitude and 51°53'04.63" W longitude in Presidente Venceslau, western São Paulo State, Brazil. The region's climate is classified as Aw (tropical with a dry winter season) according to the Köppen classification system, with an average altitude of 329 m. Rainfall data were collected on-site using a rain gauge, as shown in Figure 1. Temperature data were obtained from the Meteorological Station of the University of Oeste Paulista (Unoeste) in Presidente Prudente, SP, for the years between 2021–2023.

The soil in the study area was classified as Red-Yellow Argisols, deep, with a gently undulating to undulating relief (Rossi, 2017). Soil samples were collected from the 0–20 cm depth layer across the entire area, yielding the following average results: clay content, 6.94 kg $^{-1}$; silt, 6.24 kg $^{-1}$; sand, 86.81 kg kg^{-1}; pH (CaCl$_2$), 5.34; organic matter (O.M.), 7.54 mmolc dm^{-3}; P, 3.35 mg dm^{-3}; K, 0.32 mg dm^{-3}; Ca, 1.40 mg dm^{-3}; Mg, 0.84 mg dm^{-3}; Al, 0.13 Cmolc dm^{-3}; H + Al, 2.12 Cmolc dm^{-3}; cation exchange capacity (CEC), 4.69 mg dm^{-3}; and base saturation (V), 54.49%.

The study followed precision agriculture principles, utilizing a sampling grid with approximately four samples per hectare (4:1). Sampling points were spaced every 50 m, with adjustments made to avoid boundaries, erosion-prone areas, and tree locations.

The study area was already divided into six distinct pasture paddocks. Pastures were treated as closed units, separated from other areas. Three pasture areas (Pastures 3, 4, and 5) were planted with *Panicum maximum* cv. Mombaça (*Megathyrsus maximus* cv. Mombaça), while the other three (Pastures 1, 2, and 6) were planted with *Brachiaria brizantha* cv. MG-4, grasses belonging to the genus *Urochloa* (syn. *Brachiaria*).

Pasture 1 contained MG-4 forage, covering a total area of 4.56 ha, with 18 sampling points during the first two collections in 2022 and 17 points in the 2023 collections. The reduction in sampling points resulted from the producer's reformation of the pasture with *Brachiaria brizantha* cv. Marandu. In September 2022, conventional soil tillage was conducted in this pasture using a disc plow and leveling harrow, followed by the application of 1.3 Mg ha^{-1} of limestone, 500 kg ha^{-1} of gypsum, 250 kg ha^{-1} of simple superphosphate, 150 kg ha^{-1} of NPK 20-10-10.

Figure 1 - Rainfall and temperature data
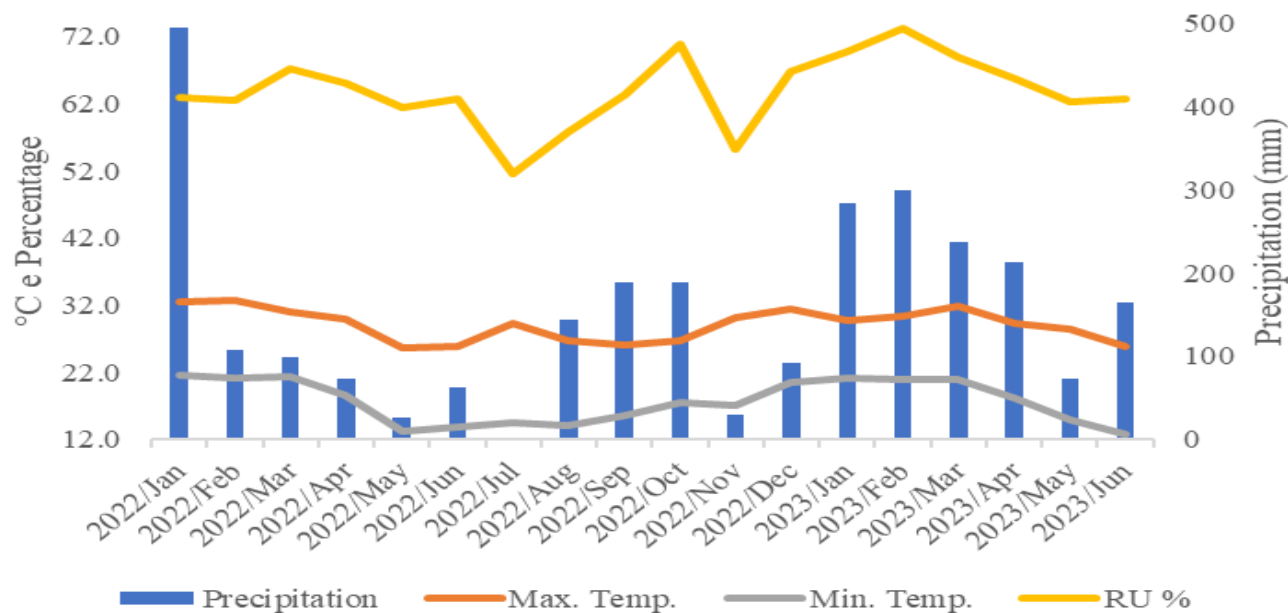
Pasture 2 contained MG-4 forage, covering a total area of 3.26 ha, with 14 sampling points.

Pasture 3 contained Mombaça forage, covering a total area of 4.0 ha, with 16 sampling points. In January 2022, 150 kg ha⁻¹ of NPK 00-20-00 was applied as topdressing, followed by 100 kg ha⁻¹ of urea in February.

Pasture 4 contained Mombaça forage, covering a total area of 2.74 ha, with 15 sampling points.

Pasture 5 contained Mombaça forage, covering a total area of 3.12 ha, with 14 sampling points.

Pasture 6 contained MG-4 forage, with a total area of 3.53 ha and 18 sampling points.

Forages were assessed at each georeferenced point for four parameters: forage height; chlorophyll content measured with an atLeaf® CHL Plus Chlorophyll Meter, which was converted to SPAD values using the website https://www.atleaf.com/SPAD, following the method of Zhu, Tremblay, and Liang (2012); and forage dry mass, determined from a representative area of 0.5×0.50 m (0.25 m²) dried in an oven at 65°C for 72 hours or until reaching constant mass. The amount of exposed soil was evaluated using an adaptation of the method proposed by Laflen, Amemiya, and Hintz (1981).

A Phantom 3 Standard drone equipped with a 1/2.3" CMOS camera (12 MP effective pixels) was used to capture images of the study area on the following dates: 01/12/2022 (summer), 07/07/2022 (winter), 08/01/2023 (summer), and 07/14/2023 (winter).

Flights were conducted at a height of 120 m with 75% frontal overlap and 65% lateral overlap. Flight planning applications included DroneDeploy® in 2022 and Drone Harmony® in 2023. The collected images were processed using WebODM (OpenDroneMap, 2020) to generate an orthomosaic map with georeferenced RGB information.

Normalized Difference Vegetation Index (NDVI) was derived from Sentinel-2 satellite images, with pre-corrected (L2A) images downloaded for the dates: 01/10/2022, 07/06/2022, 01/15/2023, and 07/14/2022. After unzipping the image folders, the data were accessed and processed using the free QGIS software (2024) to produce vegetation index maps.

NDVI classes were interpreted according to Chedid, Cortez, and Arcoverde (2024) as follows: ≤ 0.20 (Class 1), indicating exposed soil and straw; 0.20–0.40 (Class 2), indicating straw and the beginning of vegetative development; 0.40–0.60 (Class 3), indicating partial vegetative development; 0.60–0.80 (Class 4), indicating vegetative development; and > 0.80 (Class 5), indicating full development.

The GLI (Green Leaf Index) and GRVI (Green-Red Vegetation Index) were calculated for each evaluation period using the drone's RGB images, producing values ranging from -1 to 1. Quartiles were employed as the classification method, with the "Discrete Method" interpolator defining five classes. To ensure consistent classification across all maps, quartile-derived class values were averaged over the four periods, maintaining uniform classification thresholds for each index. For GLI, the following classification ranges were established: ≤ -0.02; -0.02 to 0.01; 0.01 to 0.02; 0.02 to 0.05;

and > 0.05. For GRVI, the ranges were defined as: ≤ -0.17; -0.17 to -0.14; -0.14 to -0.11; -0.11 to -0.08; and > -0.08.

Pasture Vegetation Cover (PVC) was calculated following the method of Gao *et al.* (2006). PVC was classified into five degradation categories based on its values: (1) non-degraded pasture (PVC > 90%), (2) slightly degraded pasture (90% ≥ PVC > 75%), (3) moderately degraded pasture (75% ≥ PVC > 60%), (4) seriously degraded pasture (60% ≥ PVC > 30%), and (5) extremely degraded pasture (PVC ≤ 30%). The PVC formula was adapted for the RGB indices (GLI and GRVI) used in this study, generating PVC values for each evaluation period.

Interpolation was performed to create maps of PVC for the MG-4 and Mombaça forages, using the Smart-Map plugin (Pereira *et al.*, 2022) in QGIS (QGIS.org, 2024). This plugin applies geostatistical methods, including Kriging, for spatial interpolation.

Based on the vegetation indices (VIs) and PVC data extracted from the maps, the mean, standard deviation, and coefficient of variation were then calculated. Raster files of the vegetation indices were reclassified into categories using the "*Reclassify by Table*" command in QGIS (QGIS.org, 2024). The area of each class was then determined using the GRASS "*r.report*" command in QGIS, which generates an output file listing the areas for each raster class.

Finally, the Kappa index (Cohen, 1960) was calculated to compare the generated maps. This was achieved using the GRASS "*rkappa*" function in QGIS.

RESULTS AND DISCUSSION

Table 1 presents the descriptive statistics of pasture parameters evaluated for the periods: January and July 2022 (first year), and January and July 2023 (second year).

The highest pasture height values were recorded in July of both years, attributed to forage growth driven by summer and fall rainfall (Table 1). In contrast, pasture height was lower in January due to drought conditions, as minimal rainfall from July to January creates the most challenging period for livestock in the Southeast and Midwest regions.

Table 1 - Descriptive statistics of pasture parameters

			Parameter		
Period	Average	SD[1]	Minimum	Maximum	CV[2] (%)
Plant height (cm)					
January 2022	9.36	3.02	4.75	17.50	32.26
July 2022	16.46	7.67	4.25	43.75	46.59
January 2023	12.53	7.80	4.75	31.75	62.25
July 2023	16.81	5.96	7.00	34.00	35.45
Chlorophyll (SPAD)					
January 2022	28.90	3.77	20.02	37.84	13.04
July 2022	24.13	3.89	14.94	33.80	16.12
January 2023	25.97	5.75	16.68	40.49	22.14
July 2023	22.49	3.58	14.40	34.08	15.91
Amount of exposed soil (%)					
January 2022	12.18	6.27	2	35	51.47
July 2022	9.79	7.95	0	39	81.20
January 2023	22.36	11.70	0	56	52.32
July 2023	10.77	9.49	0	40	88.11
Dry mass (kg ha-[1])					
January 2022	775.01	217.23	198.8	1393.2	28.02
July 2022	1533.87	559.94	635.6	3205.2	36.50
January 2023	955.97	424.75	318.4	2281.6	44.43
July 2023	1940.83	1020.29	577.6	4238.8	52.56

Source: The author (2023). ([1]) SD: standard deviation; ([2]) CV (%): coefficient of variation

Chlorophyll (SPAD) values were higher in January, reflecting the emergence of new leaves and shoots. In July, these values declined due to the reduced presence of young leaves and an increased proportion of senescent and dry leaves. Lower chlorophyll levels indicate reduced photosynthesis, resulting from a lower chloroplast concentration in the leaves (Table 1).

The percentage of exposed soil was more pronounced during the dry period, driven by reduced forage production, which increased the area of exposed soil in the pastures (Table 1). This exposure leads to soil loss and reduced fertility during the rainy season. High rainfall from January onward exacerbates the issue, as surface runoff carries soil material away.

Pasture dry mass production (Table 1) was higher in July, reflecting dry matter produced during the previous summer and fall. In 2023, dry mass production increased due to pasture renovation at the end of 2022.

Coefficients of variation (CVs) ranged from 13.04% to 88.11%, categorized as very high (> 30%), high (20–30%), medium (10–20%), and low (< 10%) according to Gomes (2009). Chlorophyll content (SPAD) exhibited better consistency, with medium to high CV% values (Table 1).

Height maps for MG-4 forage indicated the best results in July 2022 for pasture 6, January 2023 for pasture 1, and July 2023 for pastures 1 and 6. These findings were influenced by the renovation of pasture 1 and reduced grazing pressure on pasture 6 due to its location across a stream, which made access more difficult for animals.

Pastures on the property showed greater height and mass values in July (Figure 2), which can be attributed to rainfall accumulation during the wet season. In contrast, January values were lower due to reduced water availability before the sampling period.

These comparisons vary by region, as observed by Hott *et al.* (2016), who reported balanced pasture growth in late spring (September 22 to December 21) in tropical regions of Minas Gerais, where precipitation is well-distributed during spring. The authors also noted that areas with low pasture growth remained high throughout the study period, indicating low photosynthetic activity—a sign of degradation caused by overgrazing, erosion, low soil fertility, and adverse soil and climatic conditions.

In this sense, canopy height is a key indicator of forage mass production and is typically measured in centimeters. Even in homogeneous pastures, variations in height and dry mass occur within the forage canopy strata. Mello *et al.* (2021) noted that Mombaça pastures are impacted by grazing intensity, recommending a residue height of 45.2 cm to ensure adequate dry mass production, sufficient leaf blade availability, and a reduced proportion of

stems and dead material. In this study, the average pasture height was 16.8 cm, significantly below the recommended grazing height due to inadequate management.

The Mombaça forage height maps showed the best results for pasture 3 in July 2022 and pasture 5 in July 2023 (Figure 2). The improved performance in pasture 3 was due to maintenance fertilization applied in January 2022, while pasture 5 benefited from better grazing management, where animals spent less time grazing.

Chlorophyll index maps for MG-4 forage indicated that, in January 2023, pasture 1 exhibited most areas with a chlorophyll index between 30 and 35 SPAD (Figure 3). The high values were attributed to pasture renovation, including soil corrections and fertilization for the establishment of Marandu grass. This resulted in leaves with darker green shades, indicative of higher chlorophyll content.

The chlorophyll index maps for Mombaça forage showed a reduction in index values over time (Figure 3), with the highest values observed in January 2022 for pastures 3, 4, and 5. This decline is attributed to the forage's high soil fertility requirements, coupled with the absence of maintenance fertilization and improper management of grazing entry and exit heights.

The maps of exposed soil percentage revealed that January 2023 had the highest amount of exposed soil (Figure 4), particularly in pasture 1. This was primarily due to the pasture not being fully established at the time of collection following the renovation process.

Figure 2 - Forage height spatialization map for MG4 (1, 2, and 6) and Mombasa (3, 4, and 5) during the evaluated seasons (Jan – January and Jul – July)
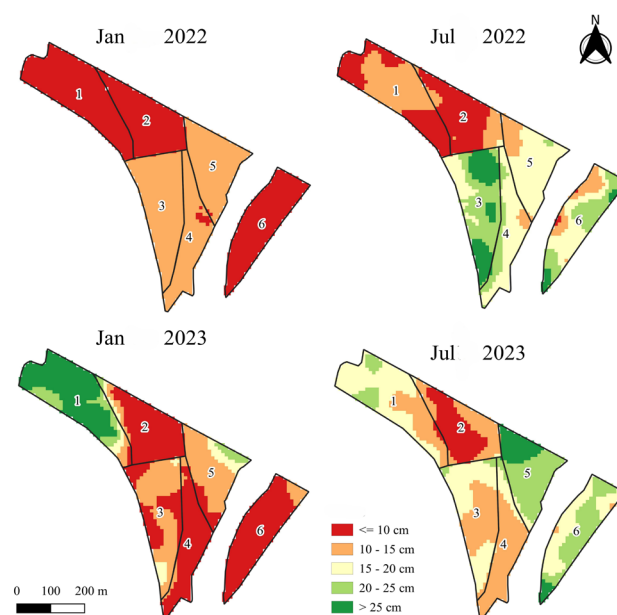
Figure 3 - Spatialization map of chlorophyll index, with the legend in SPAD units and total chlorophyll content, for forages MG4 (1, 2, and 6) and Mombaça (3, 4, and 5) during evaluation seasons (Jan – January and Jul – July)
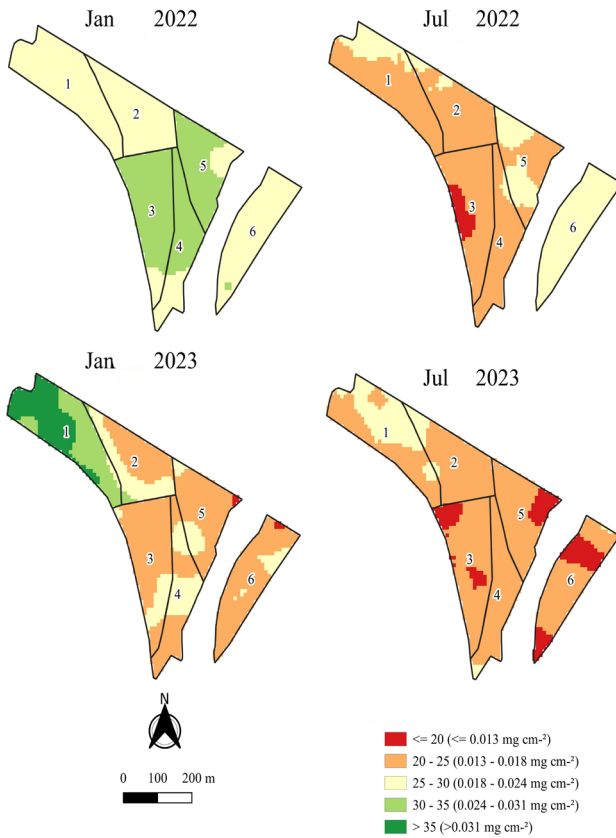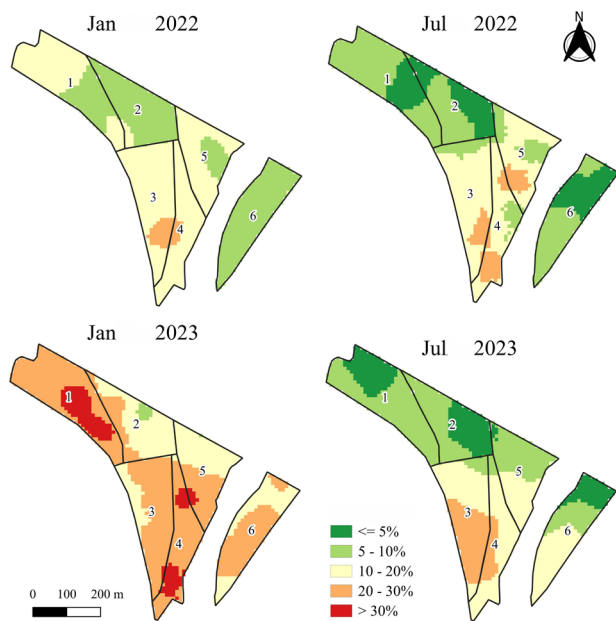

Legend:
- <= 20 (<= 0.013 mg cm⁻²)
- 20 - 25 (0.013 - 0.018 mg cm⁻²)
- 25 - 30 (0.018 - 0.024 mg cm⁻²)
- 30 - 35 (0.024 - 0.031 mg cm⁻²)
- > 35 (>0.031 mg cm⁻²)

Spatialized dry mass values for pastures with MG-4 forage indicate that only in July 2023 did pasture 3 achieve a higher dry mass yield, ranging between 2000 and 3000 kg ha⁻¹ (Figure 5). In other seasons and pastures, the values were lower, indicating a limited forage supply for the animals. Similarly, in a 2019 experiment by Freitas *et al.* (2022), conducted after a soybean harvest with *Urochloa ruziziensis* and *Pennisetum glaucum* sown in April 2019, dry mass values of approximately 1055.2 kg ha⁻¹ were reported.

The dry mass of Mombaça forage was highest in July 2023 for pasture 5 (Figure 5). In other seasons and pastures, the values remained below 2000 kg ha⁻¹. This increase occurred because the pasture was allowed to rest and recover, serving as a forage reserve for animals during the critical dry period before the onset of rains in October.

The general vegetation index, NDVI, showed better performance in 2023, with identical values of 0.54 in both January and July. During the experiment, NDVI values ranged from 0.21 (minimum) to 0.83 (maximum) (Table 2). The NDVI values were classified as having moderate variability (CV%) according to Gomes (2009), except for January 2023, which exhibited high variability.

The vegetation indices GLI and GRVI showed higher values in January for both years, except for the RI, which exhibited better values in July (Table 2). The coefficients of variation for vegetation indices calculated from drone images using the visible band (RGB) were classified as very high and high, according to Gomes (2009).

Figure 4 - Spatial maps of exposed-soil percentage for MG4 (1, 2, and 6) and Mombaça (3, 4 and 5) forages during evaluation periods (Jan – January and Jul – July)

Legend:
- <= 5%
- 5 - 10%
- 10 - 20%
- 20 - 30%
- > 30%

Figure 5 - Spatial maps of dry mass for MG4 (1, 2, and 6) and Mombaça (3, 4, and 5) forages during evaluation periods (Jan – January and Jul – July)
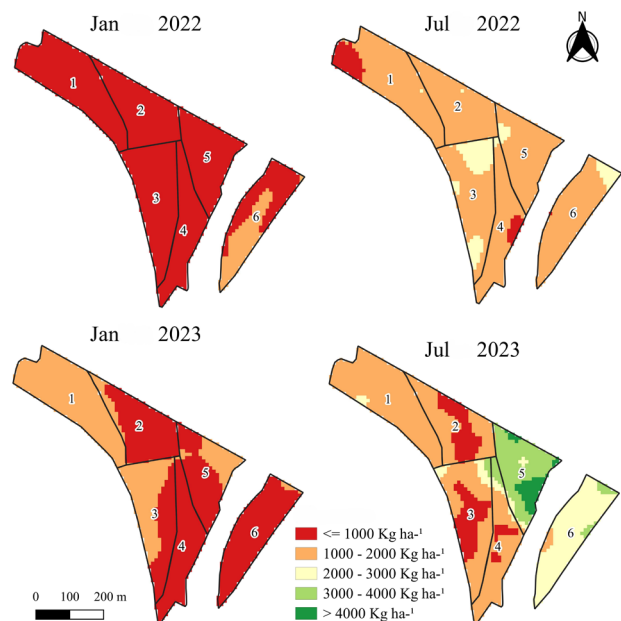

Legend:
- <= 1000 Kg ha⁻¹
- 1000 - 2000 Kg ha⁻¹
- 2000 - 3000 Kg ha⁻¹
- 3000 - 4000 Kg ha⁻¹
- > 4000 Kg ha⁻¹

Table 2 - Descriptive statistics of vegetation indices

Period	Average	SD[1]	Minimum	Maximum	CV[2] (%)
			Parameter		
			NDVI – Sentinel 2		
January 2022	0.49	0.08	0.22	0.83	16.32
July 2022	0.39	0.04	0.21	0.65	10.25
January 2023	0.54	0.11	0.26	0.81	20.37
July 2023	0.54	0.06	0.27	0.80	11.11
			GLI		
January 2022	0.01	0.048	-0.32	0.58	480
July 2022	-0.00	0.038	-0.32	0.35	0
January 2023	0.04	0.050	-0.22	0.39	12.50
July 2023	-0.002	0.040	-1.00	0.27	-2000
			GRVI		
January 2022	-0.09	0.067	-0.54	0.39	-74.44
July 2022	-0.12	0.054	-0.55	0.28	-45.00
January 2023	-0.09	0.048	-0.43	0.17	-53.33
July 2023	-0.19	0.042	-1.00	1.0	-22.10
			RI		
January 2022	0.09	0.067	-0.39	0.54	74.44
July 2022	0.12	0.054	-0.28	0.55	45.00
January 2023	0.09	0.048	-0.16	0.43	53.33
July 2023	0.19	0.042	-1.00	1.00	22.10

Source: Author (2023). ([1]) SD: standard deviation; ([2]) CV (%): coefficient of variation

The NDVI vegetation index, shown in Figure 6, indicates the highest values occurred in January. In contrast, July values were lower due to foliage being in a state of water stress and senescence.

The GLI (Figure 7) and NDVI (Figure 6) indices exhibited similar patterns, while the GRVI index (Figure 8) showed an inverse trend. In January 2023, the four vegetation indices displayed comparable patterns, with slight variations in NDVI values for pasture 6, as derived from satellite images.

Zhumanova *et al.* (2018) also observed differences in NDVI values in various ecozones, including alpine ecozones, mountainous steppes, subalpine meadow steppes, and semi-deserts, at the start of the growing season. These differences were consistent under both dry and normal conditions across all ecozones. Similarly, in this study, variations in vegetation indices align with differing precipitation levels between 2022 and 2023 (Figure 1).

The Kappa calculation (Table 3) for vegetation indices showed the highest accuracy for the NDVI x GLI relationship in July of both years. For the NDVI x GRVI relationship, Kappa values ranged from 22.03% to 24.86%, except for July 2023, which had a significantly lower Kappa value of 2.6%. For the NDVI x RI relationship, the highest accuracy values were observed from January 2022 to January 2023, with notably lower values recorded in July 2023.

When comparing GLI and GRVI in January 2023, the Kappa index accuracy was 67.23%. Using NDVI, GLI, and GRVI images enabled the identification of areas preferred by animals for grazing. Batista *et al.* (2020) observed similar results in the NDVI class intervals of thematic maps, identifying areas with higher pasture productivity and likely grazing preferences based on reductions in vegetation index values.

Due to their higher resolution, drone-derived vegetation indices allowed for the identification of

specific sparse areas. Silva, Elias, and Rosário (2022) demonstrated that GLI was sensitive to changes in plant coloration in soybean fields. During the first flight, flaws in planting, areas of healthy vegetation, and exposed soil were visible. By the second flight, regions with higher reflectance primarily corresponded to weakened vegetation.

Pasture vegetation cover was categorized into classes, with areas for each class calculated (Table 22). The predominant class was class 4, representing vegetation cover (PVC) of 60 ≥ PVC > 30%, indicative of severely degraded pasture. However, in July 2023, the GLI index showed a shift, with a larger area classified as class 3, indicative of moderately degraded pasture. This change was attributed to negative pixel values observed in the data (Table 4).

In the Kappa calculation comparing PVC derived from NDVI with PVC from other indices, assertiveness values ranged from 46.45% to 84.40%, with a notably low value of 2.64% in July 2023. Overall, there was a strong relationship between PVC from NDVI and PVC from the other indices—GLI, GRVI, and RI (Table 5). The more accurate Kappa values for PVCs derived from vegetation indices (VIs) can be attributed to the formula being applied on a positive scale from 0 to 100%, making it more suitable for comparisons between indices with extreme values.

The Kappa value for the NDVI x GLI relationship in July 2023 was the lowest, with an accuracy of 2.64%. This discrepancy may have been caused by the GLI results for this period, which differed significantly from other periods. A negative pixel value for GLI in July 2023 likely altered the entire map, as the presence of a negative value increased the overall range of values.

Figure 6 - Spatial map of NDVI vegetation index during evaluation periods (Jan – January and Jul – July)
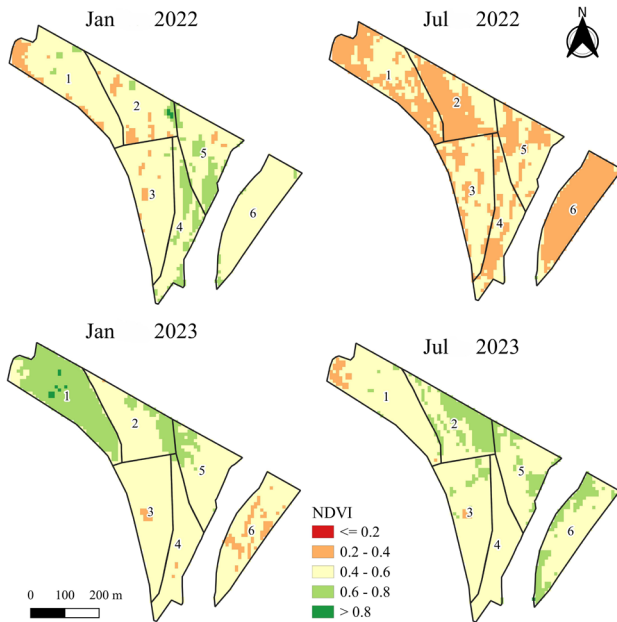

Figure 7 - Spatial map of GLI vegetation index during evaluation periods (Jan – January and Jul – July)
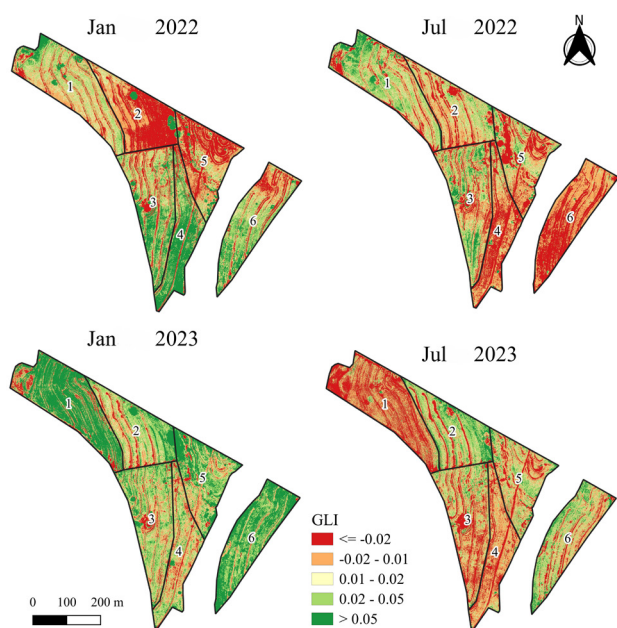

Figure 8 – Spatial map of GRVI vegetation index during evaluation periods (Jan – January and Jul – July)
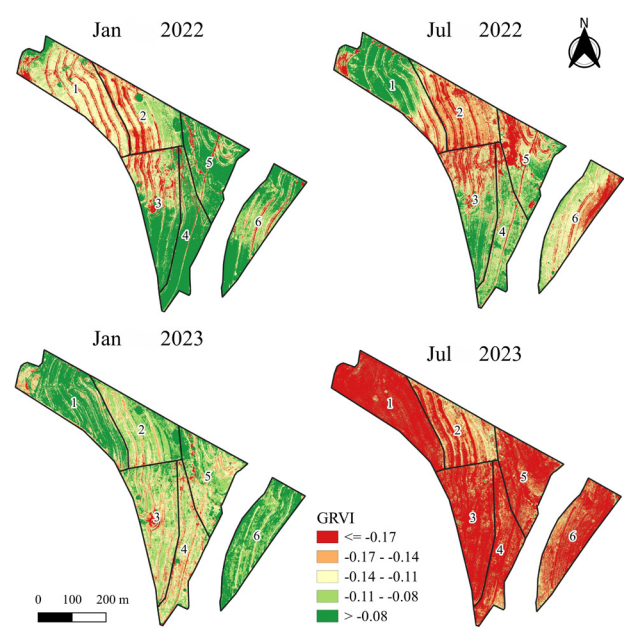
Table 3 - Kappa calculation for vegetation indices

Index		Parameter	
		Kappa	Hits (%)
NDVI x GLI	January 2022	0.008	12.59
	July 2022	0.017	24.05
	January 2023	-0.02	12.50
	July 2023	0.04	16.60
NDVI x GRVI	January 2022	0.016	23.08
	July 2022	0.015	22.03
	January 2023	0.009	24.86
	July 2023	-0.02	2.60
GLI X GRVI	January 2022	0.28	41.86
	July 2022	0.11	28.90
	January 2023	0.56	67.23
	July 2023	0.05	32.28

Source: Author (2023)

Table 4 - Calculation of area (ha) of vegetation cover class for evaluated pastures

Index	Class (ha)					
	5	4	3	2	1	Total
NDVI						
January 2022	1.38	16.80	2.62	0.27	0.06	21.13
July 2022	2.58	17.97	0.54	0.03	0.01	21.13
January 2023	2.51	13.10	1.72	2.11	1.69	21.13
July 2023	0.63	15.49	4.53	0.47	0.01	21.13
Medium	0.26	19.69	1.02	0.16	0.00	21.13
GLI						
January 2022	1.98	19.17	0.02	0.00	0.00	21.17
July 2022	0.18	20.79	0.20	0.00	0.00	21.17
January 2023	0.55	19.56	1.04	0.01	0.00	21.16
July 2023	0.00	0.01	2.31	18.83	0.00	21.15
Medium	0.00	20.90	0.25	0.00	0.00	21.15
GRVI						
January 2022	0.09	19.76	1.29	0.03	0.00	21.17
July 2022	0.09	19.76	1.29	0.03	0.00	21.17
January 2023	0.01	16.15	4.30	0.71	0.00	21.17
July 2023	0.04	21.13	0.00	0.00	0.00	21.17
Medium	0.00	21.07	0.07	0.00	0.00	21.14

Source: Author (2023). Four pasture degradation classes (Ferreira and Ferreira Neto, 2018) were defined based on PVC: (1) non-degraded pasture (CVP > 90%), (2) slightly degraded pasture (90 ≥ CVP > 75%), (3) moderately degraded pasture (75 ≥ CVP > 60%), (4) seriously degraded pasture (60 ≥ CVP > 30%) and (5) extremely degraded pasture (CVP ≤ 30%)

Table 5 - Kappa calculation for pasture vegetation cover for NDVI and other RGB indices

Index		Parameter	
		Kappa	Hits (%)
NDVI x GLI	January 2022	0.04	74.02
	July 2022	0.04	84.40
	January 2023	0.07	61.05
	July 2023	-0.02	2.64
NDVI x GRVI	January 2022	0.15	78.85
	July 2022	0.02	79.17
	January 2023	0.18	58.78
	July 2023	0.03	73.94

Source: Author (2023)

CONCLUSIONS

1. The use of UAVs for analyzing pasture development proved to be a fast and effective tool for decision-making, enabling the generation of highly detailed maps compared to satellite images. Orthomosaic images provided essential information for distinguishing pasture quality with greater precision;

2. Pasture vegetation cover (PVC), derived from NDVI, GRVI, and GLI indices, indicated slightly degraded pastures during the 2022/2023 period;

3. PVC, used as an indicator of pasture quality, was effective for the proposed study, as confirmed by the Kappa values;

4. The application of UAVs in livestock farming is highly valuable for identifying areas of lower grazing activity and exposed soil. This information aids in decision-making regarding pasture rotation and the adoption of improved management strategies.

REFERENCES

ANDRADE, R. G. *et al*. Avaliação das condições de pastagens no cerrado brasileiro por meio de geotecnologias. **Revista Brasileira de Agropecuária Sustentável**, v. 7, n. 1, p. 34-41, 2017. DOI: https://doi.org/10.21206/rbas.v7i1.376.

BATISTA, P. H. D. *et al*. Hydro-physical properties of soil and pasture vegetation coverage under animal trampling. **Revista Brasileira de Engenharia Agrícola e Ambiental**, v. 24, n. 12, p. 854-860, 2020. DOI: https://doi.org/10.1590/1807-1929/agriambi.v24n12p854-860.

CHEDID, V.; CORTEZ, J. W.; ARCOVERDE, S. N. S. Monitoring the vegetative state of coffee using vegetation indices. **Engenharia Agrícola**, v. 44, e20220212, 2024. DOI: https://doi.org/10.1590/1809-4430-Eng.Agric.v44e20220212/2024.

COHEN, J. A coefficient of agreement for nominal scales. **Educational and Psychological Measurement**, v. 20, p. 37-46, 1960. DOI: https://doi.org/10.1177/001316446002000104.

FERREIRA, G. C. V.; FERREIRA NETO, J. A. N. Uso de geoprocessamento na avaliação de degradação de pastagem no assentamento da ilha do coco, Nova Xavantina-Mato Grosso, Brasil. **Revista Engenharia Na Agricultura**, v. 26, p. 140-148, 2018. DOI: https://doi.org/10.13083/reveng.v26i2.894.

FREITAS, R. G. *et al*. Estimating pasture aboveground biomass under an integrated crop-livestock system based on spectral and texture measures derived from UAV images. **Computers and Electronics in Agriculture**, v. 198, p. 107122, 2022. DOI: https://doi.org/10.1016/j.compag.2022.107122.

GAO, Q. *et al*. Grassland degradation in Northern Tibet based on remote sensing data. **Journal of Geographical Sciences**, v. 16, n. 2, p. 165-173, 2006. DOI: https://doi.org/10.1007/s11442-006-0204-1.

GOMES, F. P. **Curso de estatística experimental**. 15. ed. Piracicaba: FEALQ, 2009. 451 p.

HERNÁNDEZ-LÓPEZ, D. *et al*. Design of a local nested grid for the optimal combined use of Landsat 8 and Sentinel 2 data. **Remote Sensing**, v. 13, n. 8, 1546, 2021. DOI: https://doi.org/10.3390/rs13081546.

HOTT, M. C. *et al*. Vegetative growth of grasslands based on hyper-temporal NDVI data from the Modis sensor. **Pesquisa Agropecuária Brasileira**, v. 51, n. 7, p. 858-868, 2016. DOI: https://doi.org/10.1590/S0100-204X2016000700009.

IBGE. **Censo agropecuário 2017**: resultados preliminares. Rio de Janeiro, 2018. Available at: https://censoagro2017.ibge.gov.br/. Accessed on Jan 26, 2024.

LAFLEN, J. M.; AMEMIYA, M.; HINTZ, E. A. Measuring crop residue cover. **Journal of Soil and Water Conservation**, v. 36, p. 341-343, 1981.

LIMA, R. P. *et al*. Changes in soil compaction indicators in response to agricultural field traffic. **Biosystems Engineering**, v. 162, p. 1-10, 2017. DOI: https://doi.org/10.1016/j.biosystemseng.2017.07.002.

MELLO, M. dos. S. de. *et al*. Comportamento de vacas mestiças em pastejo de capim Mombaça e características de forragem no semiárido. **Pubvet**, v. 15, n. 3, p. 1-10, 2021. DOI: https://doi.org/10.31533/pubvet.v15n03a763.1-10.

MORAIS, L. F. de *et al*. Avanços na avaliação de pastagens cultivadas com forrageiras tropicais no Brasil: uma revisão. **Pesquisa Aplicada & Agrotecnologia**, v. 11, n. 2, p. 125-136, 2018.

OpenDroneMap Authors ODM. **A command line toolkit to generate maps, point clouds, 3D models and DEMs from drone, balloon or kite images**. OpenDroneMap/ODM GitHub Page 2020. Available at: https://github.com/OpenDroneMap/ODM. Accessed on Feb 08, 2024.

PEREIRA, G. W. *et al.* Smart-Map: an open-source QGIS plugin for digital mapping using machine learning techniques and ordinary kriging. **Agronomy**, v. 12, e1350, 2022. DOI: https://doi.org/10.3390/agronomy12061350.

QGIS.org. 2024. **QGIS Geographic Information System**. QGIS Association. Available at: http://www.qgis.org. Accessed on Feb 08, 2024.

RAMADHANI, F. *et al*. Mapping a cloud-free rice growth stages using the integration of PROBA-V and Sentinel-1 and its temporal correlation with sub-district statistics. **Remote Sensing**, v. 13, n. 8, e1498, 2021. DOI: https://doi.org/10.3390/rs13081498.

ROSSI, M. **Mapa pedológico do Estado de São Paulo**: revisado e ampliado. São Paulo: Instituto Florestal, 2017. 118 p.

SANTOS, P. S.; FERREIRA, L. G.; LENZI, Í. L. C. Caracterização biofísica das pastagens na bacia hidrográfica do Rio Vermelho-GO, bioma cerrado, Brasil. **Boletim de Geografia**, v. 36, n. 3, p. 53-73, 2018. DOI: https://doi.org/10.4025/bolgeogr.v36i3.35269.

SILVA, L. C. A. Delineamento de zonas de manejo por imagens suborbitais, orbitais e variáveis de solo. 2020. 117 f. Dissertação (Mestrado em Engenharia Agrícola) – Universidade Estadual do Oeste do Paraná, Cascavel, PR, 2020.

SILVA, M. H. da; ELIAS, A. R.; ROSÁRIO, L. L. do. Análise da cultura da soja a partir de índices de vegetação (ExG - GLI - TGI - VEG) advindos de imagens RGB obtidas com ARP. **Revista Brasileira de Geomática**, v. 10, n. 2, p. 140-154, 2022. DOI: 10.3895/rbgeo.v10n2.15042.

THEMISTOCLEOUS, K. *et al*. Use of remote sensing and UAV for the management of degraded ecosystems: the case study of overgrazing in Randi Forest, Cyprus. **International Society for Optics and Photonics**, v. 9229, 2014. DOI: https://doi.org/10.1117/12.2069515.

WEISS, M.; JACOB, F.; DUVEILLER, G. Remote sensing for agricultural applications: a meta-review. **Remote Sensing of Environment**, v. 236, e111402, 2020. DOI: https://doi.org/10.1016/j.rse.2019.111402.

ZHU, J.; TREMBLAY, T.; LIANG Y. Comparing SPAD and atLEAF values for chlorophyll assessment in crop species. **Canadian Journal of Soil Science**, v. 92, p. 645-648, 2012. DOI: https://doi.org/10.1139/CJSS2011-100.

ZHUMANOVA, M. *et al.* Assessment of vegetation degradation in mountainous pastures of the Western Tien-Shan, Kyrgyzstan, using eMODIS NDVI. **Ecological Indicators**, v. 95, p. 527-543, 2018.